# DC resistivity modeling based on spectral element method with unstructured grids

*Jiao Zhu[1,2]*, Changchun Yin[1], Yunhe Liu[1]*

1.College of Geo-exploration Science and Technology, Jilin University, Changchun , China
2. Institute of Geophysics and Meteorology, University of Cologne, Cologne, Germany
*Contact: zhujiaojlu@163.com

## Introduction

In finite element (FE) method, there generally exist two strategies for improving the model accuracy: to refine grids (*h-type*) and to raise the order of interpolation functions (*p-type*). Between the two strategies, the grid refinement has been more widely used, especially with the application of the adaptive unstructured FE method (Ren & Tang 2010). The other strategy, namely the high-order interpolation method including spectral element method (SEM) is combined with the finite element method and the spectral method. The classic SEM uses the Gauss-Lobatto-Legendre (GLL) polynomials for interpolation functions with the numerical integration realized on GLL nodes. In this way, one can obtain a diagonal mass matrix for the modeling and enhancing precision (Komatitsch & Tromp 1999). Since GLL polynomials can only be applied to rectangular or hexahedron, to fit irregular interfaces, one needs to use triangle or tetrahedron element which can well model the complex interfaces with relatively homogeneous grids. This stimulates the research to develop a spectral element method based on tetrahedral grids (TSEM). Meanwhile, the spectral element method can be applied to the 3D forward modeling DC resistivity method for verifying its effectiveness.

## Theory

**Tetrahedral spectral element method (TSEM)**

**Basis function** (*n*-th order) : Proriol-Koornwinder-Dubiner (PKD)

$$\psi_N(\xi,\eta,\zeta)=\sqrt{\frac{8}{\gamma_{ijk}}}P_i^{(0,0)}\left(-2\frac{1+\xi}{\eta+\zeta}-1\right)P_j^{(2i+1,0)}\left(2\frac{1+\eta}{1-\zeta}-1\right)\left(2-2\frac{1+\eta}{1-\zeta}\right)^i P_k^{(2i+2j+2,0)}(\zeta)(1-\zeta)^{i+j}$$

Where $\gamma_{ijk}=\frac{2}{2i+1}\frac{2^{2i+2}}{2i+2j+2}\frac{2^{2i+2j+3}}{2i+2j+2k+3}$, Corresponding to the permutation of *i*, *j*, *k*, we have $\sum_{N=1}^{Nt}\Leftrightarrow\sum_{i=0}^{n}\sum_{j=0}^{n-i}\sum_{k=0}^{n-i-j}$ and $P_i^{(\alpha,\beta)}(\xi)$ are orthogonal Jacobian polynomials of *i*-th order with the orthogonal weight $w(\xi)=(1-\xi)^\alpha(1+\xi)^\beta$. PKD polynomials cannot be used directly as interpolation functions for not satisfying $\varphi_i(x_j)=\delta_{ij}$, thus a Vandermonde matrix **V** is needed to connect PKD polynomials and interpolation functions

$$\boldsymbol{\varphi}=\begin{bmatrix}\varphi_1(\mathbf{r})\\ \varphi_2(\mathbf{r})\\ \vdots\\ \varphi_{Nt}(\mathbf{r})\end{bmatrix}=\begin{bmatrix}\psi_1(\mathbf{r}_1) & \psi_2(\mathbf{r}_1) & \cdots & \psi_{Nt}(\mathbf{r}_1)\\ \psi_1(\mathbf{r}_2) & \psi_2(\mathbf{r}_2) & \cdots & \psi_{Nt}(\mathbf{r}_2)\\ \vdots & \vdots & \ddots & \vdots\\ \psi_1(\mathbf{r}_{Nt}) & \psi_2(\mathbf{r}_{Nt}) & \cdots & \psi_{Nt}(\mathbf{r}_{Nt})\end{bmatrix}^{-1}\begin{bmatrix}\psi_1(\mathbf{r})\\ \psi_2(\mathbf{r})\\ \vdots\\ \psi_{Nt}(\mathbf{r})\end{bmatrix}=(\mathbf{V}^{-1})^{\mathrm{T}}\boldsymbol{\psi}$$

where $Nt=\frac{(n+1)(n+2)(n+3)}{6}$ is the number of interpolation points in tetrahedral

**Interpolation nodes**: warp and blend nodes (Warburton 2006)

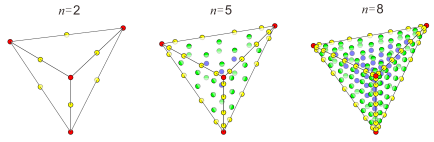


***Figure 1.*** *Distribution of interpolation nodes in a right-angle tetrahedron for the order of n=2, 5, and 8. The red points are nodes at vertexes, the yellow ones are for edge nodes, the green ones are for surface nodes, while the blue points are for interior nodes.*

| Order/*n* | 1 | 2 | 3 | 4 | 5 | 6 | 7 | 8 |
|---|---|---|---|---|---|---|---|---|
| *Nt* | 4 | 10 | 20 | 35 | 56 | 84 | 120 | 165 |
| *Ni* | 0 | 0 | 0 | 1 | 4 | 10 | 20 | 35 |

***Table 1.*** *Number of total nodes Nt and interior nodes Ni for n-th order interpolation.*

## References

**[1]** Ren, Z., & Tang, J., 2010. 3D direct current resistivity modeling with unstructured mesh by adaptive finite-element method. Geophysics, 75(1): H7-H17.
**[2]** Komatitsch, D., & Tromp, J., 1999. Introduction to the spectral-element method for 3-D seismic wave propagation. Geophysical Journal International 139(3), 806–822.
**[3]**Warburton, T., 2006. An explicit construction of interpolation nodes on the simplex. Journal of Engineering Mathematics, 56(3), 247-262.
**[4]**Wait, J. R., 1990. Current flow into a three-dimensionally anisotropic conductor. Radio Science, 25(5), 689-694.

## Numerical examples

- **Two layer model**
  **Layer 1** resistivity : 1 Ω·m thickness : 10m
  **Layer 2** resistivity : 100 Ω·m
  **Point current source**: 1A
  **Receiving points area**: 100 m ×100 m interval : 1m

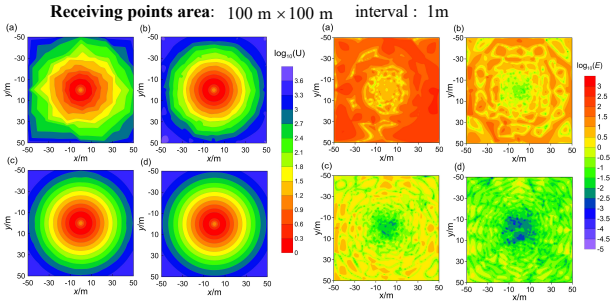

***Figure 2.*** *Electrical potentials for a point source at the surface of a 2-layer earth. The TSEM order is changing. (a) n=1 (b) n=2 (c) n=3 (d) n=4.*



***Figure 3.*** *Errors E in percentage related to the 1D analytical solutions for the model in Fig. 2 for different order of TSEM. (a) n=1 (b) n=2 (c) n=3 (d) n=4.*

In figure 2, note that with increasing order, the contours become more and more smooth and circular that is close to the true distribution of potential for a point source. Moreover, we compare our modeling results with the analytical solutions given by Wait (1990). From Fig. 3, it is seen that with the increasing order the relative errors decrease sharply. The maximum error for *n*=1 is 451.5%, while it is 2.3% for *n*=4.

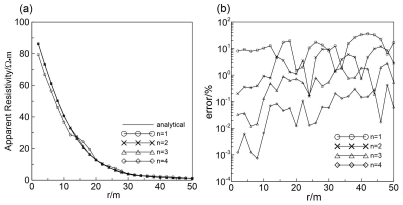

***Figure 4.*** *Modeling results of our TSEM in comparison to the analytical solutions along the profile z=0m, x=0m for the layered model given in Fig. 4. (a) Apparent resistivity; (b) relative errors.*

Meanwhile, we have chosen a profile along the y-axis to present our model results and the relative errors against the analytical solutions in Fig. 2. From the figure, we can draw the same conclusion that with increasing order in our TSEM the accuracy is vastly improved.

- **2D valley model**
  **Resistivity** : 100 Ω·m
  **Configuration**: dipole-dipole

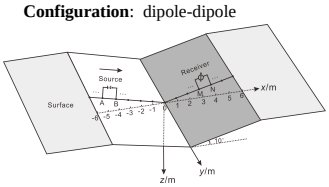


***Figure 5.*** *2D valley model*

Then we calculate the model in Fig.5 with TSEM and get the relative error with Ren & Tang (2010) in Fig. 6. When *n*=1, average relative error is 14.538%; *n*=2, relative error decreases sharply to 2.387%; for *n*=3 and *n*=4, relative error is very close, that is 1.161% and 1.044%, respectively, the numerical results almost converge. Whereas with our algorithm, TSEM also has good processing result to the terrain problem.

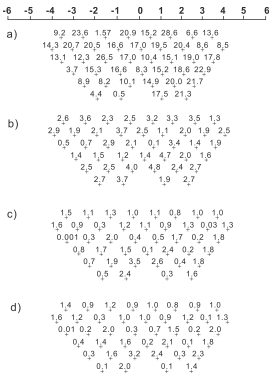

***Figure 6.*** *Relative percentage error of the apparent resistivities between different interpolation order and 2 times adaptive refined in mesh. (a) n=1 (b) n=2 (c) n=3 (d) n=4.*

## Conclusions

It is demonstrated that the method we presented about the application of TSEM to DC forward modeling is very advantageous in highly accuracy which depart from the conventional finite element method, especially suit for complex models and rough meshes.